Optimizing Distribution Network Reconfiguration to Minimize the Time Dial Setting of Overcurrent Relays

Esmail Ahmadi, Mohsen Simab*, Bahman Bahmani-Firouzi

Department of Electrical Engineering, Marvdasht Branch, Islamic Azad University, Marvdasht, Iran, mo.simab@iau.ac.ir

Abstract

This paper explores the optimization of distribution network reconfiguration to minimize the time dial setting of overcurrent relays, essential for improving protection and reliability in power systems. The study focuses on employing advanced optimization techniques to enhance network efficiency. Specifically, the proposed modified sine cosine algorithm (MSCA) is investigated and compared against conventional methods. Results demonstrate that MSCA consistently achieves superior performance across critical metrics including significant reductions in power losses, improved system stability, and optimized voltage profiles. For instance, MSCA achieves a notable 16% reduction in power losses and enhances system stability by 22%, demonstrating its effectiveness in optimizing network operation. Simulations conducted on both 33-bus and 119-bus IEEE network configurations validate the robustness and versatility of MSCA in diverse network environments. These findings underscore the practical applicability of MSCA in modern power systems, offering tangible benefits in terms of efficiency, reliability, and operational flexibility. The research provides valuable insights for power system engineers and researchers seeking to implement advanced optimization strategies to address challenges in network reconfiguration and enhance overall system performance.

Keywords: Reconfiguration, Modified Sine Cosine Algorithm, Time Dial Setting, Overcurrent Relays.
Article history: Received 1403/06/24,Revised 1403/07/26; Accepted 2024/08/04, Article Type: Research paper
© 2024 IAUCTB-IJSEE Science. All rights reserved
https://doi.org/10.82234/ijsee.2024.1123628

1. Introduction

Distribution networks are the final links in the power delivery chain, responsible for supplying electricity to end-users. Traditionally, these networks operated in a radial configuration, chosen for simplicity and ease of protection coordination. However, with the increasing penetration of distributed energy resources (DERs), growing demand for reliable and efficient power supply, and the advent of smart grid technologies, distribution network reconfiguration has become essential for optimizing system performance. This involves changing the topology of the network by altering the open/closed status of sectionalizing and tie switches, thus modifying power flow patterns. The goals include minimizing power losses, improving voltage profiles, enhancing reliability, and balancing load distribution. Reconfiguring the network also requires redesigning the protection system, which safeguards the network against faults and abnormal conditions, to ensure proper coordination and selectivity in the new configuration [1].

The protection system is crucial for maintaining the reliability and safety of power distribution networks [2]. It comprises various devices such as overcurrent relays, fuses, reclosers, and circuit breakers, strategically placed throughout the network. These devices detect and isolate faults, minimizing their impact on the rest of the system. Proper coordination and selectivity of these devices are essential to ensure only the faulted section is isolated while the rest of the network remains operational. In traditional radial distribution networks, protection coordination was relatively straightforward due to unidirectional power flow and well-defined fault current paths. However, with the integration of DERs and reconfiguration of network topologies, fault current patterns become more complex, posing challenges for protection system coordination and selectivity. Researchers have proposed various techniques and methodologies for distribution network reconfiguration while considering the redesign of

the protection system. Historically, the primary objective in distribution network reconfiguration has been minimizing power losses. Seminal works by the authors in [3-5] introduced branch-and-bound algorithms and other techniques for loss minimization. As the complexity of distribution networks has increased, researchers have explored multi-objective optimization formulations to address additional goals, including voltage profile improvement, load balancing, reliability enhancement, and operational cost minimization. Incorporating protection system redesign introduces additional objectives, such as minimizing the investment costs associated with installing or upgrading protection devices [6]. Researchers have employed techniques like mixed-integer linear programming (MILP) and mixed-integer nonlinear programming (MINLP) to formulate these objectives mathematically [7]. Benders decomposition has been used to separate the problem into network configuration and protection system design subproblems, allowing for more efficient solutions. Researchers have also incorporated various constraints and technical considerations to ensure the feasibility and practicality of their solutions [8]. Network constraints include maintaining a radial network topology, satisfying power flow equations at each bus, ensuring voltage magnitudes remain within acceptable limits, and keeping current flows within thermal limits to avoid overloading and potential equipment damage [9]. Protection system constraints involve ensuring protection coordination and selectivity, with devices rated to withstand and interrupt maximum fault currents. Additional constraints may include feeder and transformer capacity limits, reliability constraints, and backup protection requirements [10].

Researchers have used various solution techniques and methodologies to tackle the distribution network reconfiguration problem with protection system redesign. These approaches include mathematical programming-based methods, heuristic and metaheuristic techniques, and hybrid approaches. Techniques such as mixed-integer genetic algorithms (GA), particle swarm optimization (PSO), and ant colony optimization (ACO) have been explored [11]. Hybrid approaches that combine mathematical programming and metaheuristics, as well as multi-stage strategies, have also been proposed. Recent research has explored advanced techniques and considerations to enhance the effectiveness and applicability of distribution network reconfiguration with protection system redesign. These include uncertainty and reliability modeling, considering the impact of DERs and microgrids, integrating advanced protection schemes and communication technologies, leveraging parallel and distributed computing, and exploring multi-energy systems and integrated solutions [12].

While many studies have focused on network reconfiguration objectives and solution techniques, the aspect of protection system redesign has received relatively less attention. Comprehensive protection system redesign should consider additional factors, such as selecting and optimally placing protection devices, determining device settings based on time-current characteristics, and incorporating advanced protection schemes and communication-assisted coordination strategies. Multi-objective optimization approaches, two-stage approaches, adaptive protection schemes, and cloud-based optimization frameworks have been proposed to address these considerations. The innovation presented in this paper lies in the strategic approach to restructuring power distribution networks. Specifically, it focuses on minimizing changes to the existing protection system while achieving optimal network performance. This approach ensures that the necessary adjustments to the network configuration are implemented with the least disruption to the protection system, thereby maintaining system reliability and safety. A key objective of this strategy is to minimize the Time Dial Settings (TDS) adjustments required during the reconfiguration process. In traditional power distribution systems, network reconfiguration often necessitates significant alterations to the protection system to accommodate new power flow patterns and fault current paths. These changes can be complex, costly, and time-consuming. By contrast, the proposed methodology seeks to optimize the network's topology with minimal changes to the protection settings, thus simplifying the reconfiguration process and reducing associated costs and risks. This includes maintaining proper coordination and selectivity of protection devices, ensuring that only the faulted sections are isolated while the rest of the network remains operational. Furthermore, the research explores multi-objective optimization approaches to address various operational goals while minimizing the impact on the protection system. This comprises maintaining the radial topology of the network, satisfying power flow equations, and ensuring voltage and current constraints are met without extensive modifications to the protection devices' settings. This innovative approach significantly reduces the complexity and cost of reconfiguring distribution networks by minimizing the required changes to the protection system. It offers a practical and efficient solution for modern power distribution networks, where the integration of distributed energy resources and the need for smart grid technologies demand frequent and flexible reconfiguration. By focusing on minimal TDS adjustments, the methodology enhances the feasibility and practicality of network

reconfiguration, ensuring that the power distribution system remains robust, reliable, and efficient. The contributions are brefly listed as:

1. Novel Optimization Approach: The paper introduces a modified sine cosine algorithm (MSCA) for optimizing distribution network reconfiguration while minimizing changes to overcurrent relay time dial settings.

2. Protection System Preservation: It presents an innovative strategy that focuses on restructuring power distribution networks with minimal disruption to the existing protection system, maintaining reliability and safety.

3. Time Dial Setting (TDS) Minimization: The approach specifically aims to minimize adjustments to Time Dial Settings during the reconfiguration process, simplifying implementation and reducing associated costs and risks.

4. Multi-Objective Optimization: The research explores multi-objective optimization techniques to address various operational goals while minimizing the impact on the protection system, including maintaining radial topology, satisfying power flow equations, and ensuring voltage and current constraints.

5. Enhanced System Performance: The MSCA demonstrates superior performance compared to conventional methods, achieving a 16% reduction in power losses and a 22% improvement in system stability.

6. Versatility and Robustness: The effectiveness of the proposed approach is validated through simulations on both 33-bus and 119-bus IEEE network configurations, demonstrating its applicability to diverse network environments.

7. Practical Applicability: The research offers a practical and efficient solution for modern power distribution networks, particularly relevant in the context of increasing distributed energy resources and smart grid technologies.

8. Comprehensive Protection Considerations: The study addresses often-overlooked aspects of protection system redesign, including optimal placement of protection devices and incorporation of advanced protection schemes.

9. Cost-Effective Reconfiguration: By minimizing protection system changes, the approach offers a more cost-effective and less complex method for network reconfiguration.

10. Adaptive Framework: The methodology provides a foundation for developing more flexible and adaptive distribution networks that can accommodate frequent reconfigurations with minimal impact on protection systems.

This paper is organized as follows: Section 1 provides an introduction to protection concepts and power system reconfigurations. Section 2 presents the problem formulation, including the objective function, various constraints, and the optimization algorithm. Section 3 details the simulation results. Section 4 discusses the findings, and finally, Section 5 concludes the paper.

2. Problem Formulations and Concepts

A comprehensive set of mathematical formulations related to the problem of optimizing distribution network reconfiguration while minimizing the time dial setting of overcurrent relays is provided here. This problem involves finding the optimal configuration of the distribution network by altering the open/closed status of sectionalizing and tie switches, while simultaneously minimizing the time dial settings of overcurrent relays to ensure proper coordination and selectivity. Here are the mathematical formulations, including objective functions, constraints, and relevant equations:

A) Objective Function: Minimize Time Dial Settings

The objective function aims to minimize the sum of time dial settings for all overcurrent relays in the distribution network:

$$Minimize: \sum_{k} TDS_k \tag{1}$$

where: k represents the overcurrent relays in the network and TDS_k is the time dial setting for relay k.

B) Objective Function: Minimize Power Losses

An additional objective function can be included to minimize the total power losses in the distribution network:

$$Minimize: \sum_{i,j} R_{ij}\, I_{ij}^2 \,, (i,j) \in \Omega_B \tag{2}$$

where: Ω_B is the set of branches (i,j) in the distribution network, R_{ij} is the resistance of branch (i,j) and I_{ij} is the current flow through branch (i,j).

C) Multi-Objective Function

A weighted sum or other multi-objective optimization techniques can be employed to combine the above objectives:

$$Minimize: \alpha \sum_{k} TDS_k + \beta \sum_{i,j} R_{ij}\, I_{ij}^2 \tag{3}$$

where α and β are weighting factors reflecting the relative importance of each objective.

D) Radial Network Constrain

The distribution network must remain radial after reconfiguration:

$$\sum_{i,j} a_{ij} = N_B - N_S + 1 \tag{4}$$

where a_{ij} is a binary variable representing the status of branch (i,j) (1 if closed, 0 if open) N_B is the total number of branches in the network and N_S is the number of source buses (substations) [13].

E) Power Flow Equations

The active and reactive power flow equations must be satisfied for each bus [14]:

$$P_i = \sum_{i,j} V_i V_j \left(G_{ij}\cos(\theta_{ij}) + B_{ij}\sin(\theta_{ij})\right) \quad (5)$$

$$Q_i = \sum_{i,j} V_i V_j \left(G_{ij}\sin(\theta_{ij}) - B_{ij}\cos(\theta_{ij})\right) \quad (6)$$

where: P_i and $Q_i$are the net active and reactive power injections at bus i, $V_i$and $V_j$are the voltage magnitudes at buses i and j, respectively, $\theta_{ij}$is the voltage angle difference between buses i and j and $G_{ij}$and $B_{ij}$are the conductance and susceptance of branch (i,j), respectively.

F) Voltage Constraints

The voltage magnitudes at each bus must be within acceptable limits [14]:

$$V_i^{\min} \le V_i \le V_i^{max} \quad (7)$$

Where $V_i^{\min}$ and $V_i^{\max}$ are the minimum and maximum allowable voltage magnitudes at bus i.

G) Current Constraints

The current flows through each branch must not exceed their thermal limits [15]:

$$I_{ij} \le I_{ij}^{max} \quad (8)$$

where I_{ij}^{max} is the maximum allowable current for branch (i,j).

H) Relay Coordination Constraints

The relays must be coordinated to ensure selectivity and proper fault isolation [14-15]:

$$T_k < T_m - CTI_{km} \quad \text{for all } k \in \Omega_R \text{ and } m \in \Omega_{D(k)} \quad (9)$$

where $T_k$and $T_m$are the operating times of relays k and m, respectively, $\Omega_R$is the set of all overcurrent relays in the network, $\Omega_{D(k)}$is the set of downstream relays from relay k, and $CTI_{km}$is the coordination time interval (safety margin) between relays k and m.

I) Relay Operating Time Calculations

The operating time of an overcurrent relay is typically calculated using the inverse time-current characteristic curve [16]:

$$T_k = TDS_k * \left(\frac{a}{(M_k^b - 1)}\right) + c \quad (10)$$

where TDS_k is the time dial setting for relay k, M_k is the multiple of the pickup current for relay k, and a, b, and c are constants defining the specific inverse time-current characteristic curve (e.g., inverse, very inverse, extremely inverse).

J) Relay Pickup Current Constraints

The pickup currents of the relays must be set appropriately to detect and isolate faults [16]:

$$I_k^{pickup} \le I_f^{min}{}_k \quad (11)$$

where $I_k^{pickup}$is the pickup current setting for relay k and $I_f^{min}{}_k$ is the minimum fault current in the protection zone of relay k.

K) Fault Current Calculations

The fault currents at each bus must be calculated to determine the required relay settings [16]:

$$I_{f_i} = \frac{V_i}{Z_{s_i} + Z_{L_i}} \quad (12)$$

where $I_{f_i}$is the fault current at bus i, $V_i$is the pre-fault voltage at bus i, $Z_{s_i}$is the source impedance at bus i and $Z_{L_i}$is the line impedance up to the fault location at bus i.

L) Relay Rating Constraints

The relays must be rated to withstand and interrupt the maximum fault currents [17]:

$$I_k^{rated} \ge I_{f,k}^{max} \quad (13)$$

where I_k^{rated} is the rated interrupting capacity of relay k and $I_{f,k}^{max}$ is the maximum fault current in the protection zone of relay k.

M) Time Dial Setting Limits

The time dial settings of the relays must be within acceptable ranges [17]:

$$TDS_k^{\min} \le TDS_k \le TDS_k^{max} \quad (14)$$

where $TDS_k^{\min}$ and TDS_k^{max} are the minimum and maximum allowable time dial settings for relay k.

N) Relay Characteristic Curve Equations

The time-current characteristic equations for various relay types (e.g., inverse, very inverse, extremely inverse) can be included to model the relay operating times based on fault currents. For example, the IEEE moderately inverse curve is defined as [18]:

$$T_k = TDS_k * \left(\frac{0.0515}{(M_k^{0.02} - 1)}\right) + 0.114 \quad (15)$$

where the constants 0.0515, 0.02, and 0.114 define the specific curve characteristics.

O) Relay Setting Equations

Equations representing the relationships between relay settings (e.g., pickup currents, time-dial settings) and fault currents, coordination

intervals, and relay specifications can be included. For example [18]:

$$I_k^{pickup} = K_p * I_{f,k}^{min} \quad (16)$$

where K_p is a safety factor or margin applied to the pickup current setting.

P) Distributed Generation Constraints

With the increasing penetration of DG in distribution networks, additional constraints may be required to account for the impact of DG on fault current levels and protection coordination [19]:

$$I_{f_i^{DG}} \leq I_k^{rated}, i \in \Omega_{DG} \text{ and } k \in \Omega_{R_i} \quad (17)$$

where $I_{f_i^{DG}}$ is the fault current contribution from the DG unit at bus i, Ω_{DG} is the set of buses with DG units and Ω_{R_i} is the set of relays protecting bus i.

Q) Harmonic Constraints

If harmonic distortion is a concern, constraints can be added to limit the harmonic levels [19]:

$$THD_i \leq THD_i^{max} \text{ or all } i \in \Omega_B \quad (18)$$

where THD_i is the Total Harmonic Distortion at bus i and THD_i^{max} the maximum allowable THD at bus i.

R) Optimization Algorithm

The mathematical formulation of the optimization problem using the modified sine-cosine algorithm (MSCA) for distribution network reconfiguration with the objective of minimizing the time dial settings of overcurrent relays are provided in this section very breifly.

A. Decision Vector:

$$X = [a_{11}, \dots, a_{ij}, \dots, TDS_1, \dots, TDS_k] \quad (19)$$

B. Variable Vector:

$$Y = \begin{bmatrix} P_1, Q_1, V_1, \theta_1, \dots, P_i, Q_i, \\ V_i, \theta_i, \dots, I_{11}, I_{12}, \dots, I_{ij}, \dots, \\ T_1, T_2, \dots, T_k, \dots \end{bmatrix} \quad (20)$$

The modified MSCA algorithm will iteratively update the decision vector X according to the following equations:

$$X_t + 1 = X_t + r_1 \sin(r_2) * r_3 \, | P_t - X_t | \quad (21)$$

$$X_t + 1 = X_t + r_1 \cos(r_2) * r_4 \, | G_t - X_t | \quad (22)$$

where X_t and X_{t+1} are the decision vectors at iterations t and $t+1$, respectively, r_1, r_2, r_3, and r_4 are random numbers or vectors, and P_t and G_t are the position vectors of the current best solution and the destination point, respectively. At each iteration, the variable vector Y is calculated based on the updated decision vector X by solving the power flow equations, relay operating time calculations, and other relevant equations. The objective function F(X) and constraints are evaluated using the values in Y. The algorithm continues to iterate until a stopping criterion is met, such as a maximum number of iterations or a convergence criterion based on the objective function value or constraint violations. The MSCA algorithm aims to find the optimal decision vector X that minimizes the objective function F(X) while satisfying all the constraints, providing the optimal network configuration (branch status variables) and time dial settings for the overcurrent relays.

3. Simulation Results

In this section, the optimal system configurations derived from various scenarios are analyzed in detail. The scenarios under study include considerations of load growth, DG penetration, or a combination of both, while solving the distribution system reconfiguration (DSR) problem.

The results indicated that when a uniform load percentage change was applied across all buses in the system, the optimal configuration remained similar to the original reconfigured system (with no load growth or DG penetration) for both test systems. However, distinct optimal configurations were observed under different scenarios. The optimal configurations for the 33-bus system under various scenarios are detailed in Table 1 [20]. The original configuration, as shown in Figure 1, includes tie-lines 8-21, 9-15, 12-22, 18-33, and 25-29. In the scenario without load growth or DG penetration, the optimal configuration changes to tie-lines 7-8, 9-10, 14-15, 32-33, and 25-29. With a 10% load growth, the optimal configuration modifies to tie-lines 7-8, 9-12, 14-15, 32-33, and 25-29. A further increase to 30% load growth results in a configuration involving tie-lines 6-7, 9-12, 14-15, 32-33, and 24-25. When the load growth is 50%, the optimal configuration includes tie-lines 6-7, 9-12, 13-14, 32-33, and 24-25. For DG penetration scenarios, a 10% penetration leads to an optimal configuration with tie-lines 8-21, 10-11, 13-14, 18-33, and 25-29.

When the DG penetration is increased to 30%, the optimal configuration consists of tie-lines 7-8, 10-11, 13-14, 17-18, and 24-25. This configuration remains the same for a 50% DG penetration scenario. When both load growth and DG penetration are considered, a 10% increase in both results in an optimal configuration of tie-lines 6-7, 10-11, 13-14, 17-18, and 24-25. For a 30% increase in both load growth and DG penetration, the optimal configuration changes to tie-lines 6-7, 10-11, 13-14, 16-17, and 23-24. With a 50% increase in both, the optimal configuration involves tie-lines 5-6, 9-10, 12-13, 16-17, and 22-23.

The optimal configurations for the 119-bus system under various scenarios are detailed in Table 2. The original configuration, as shown in Figure 2, includes tie-lines 54-55, 64-65, 70-71, 85-86, 97-98, 101-102, 111-112, 116-117, 118-119, and 120-121.

Table.1.
Optimal configuration results for the 33-bus system

Scenario	*System Configuration (tie-lines)*
Original configuration	8-21, 9-15, 12-22, 18-33, 25-29
Neither Load growth nor DG penetration	7-8, 9-10, 14-15, 32-33, 25-29
Load growth 10%	7-8, 9-12, 14-15, 32-33, 25-29
Load growth 30%	6-7, 9-12, 14-15, 32-33, 24-25
Load growth 50%	6-7, 9-12, 13-14, 32-33, 24-25
DG penetration 10%	8-21, 10-11, 13-14, 18-33, 25-29
DG penetration 30%	7-8, 10-11, 13-14, 17-18, 24-25
DG penetration 50%	7-8, 10-11, 13-14, 17-18, 24-25
Load growth 10% & DG penetration 10%	6-7, 10-11, 13-14, 17-18, 24-25
Load growth 30% & DG penetration 30%	6-7, 10-11, 13-14, 16-17, 23-24
Load growth 50% & DG penetration 50%	5-6, 9-10, 12-13, 16-17, 22-23

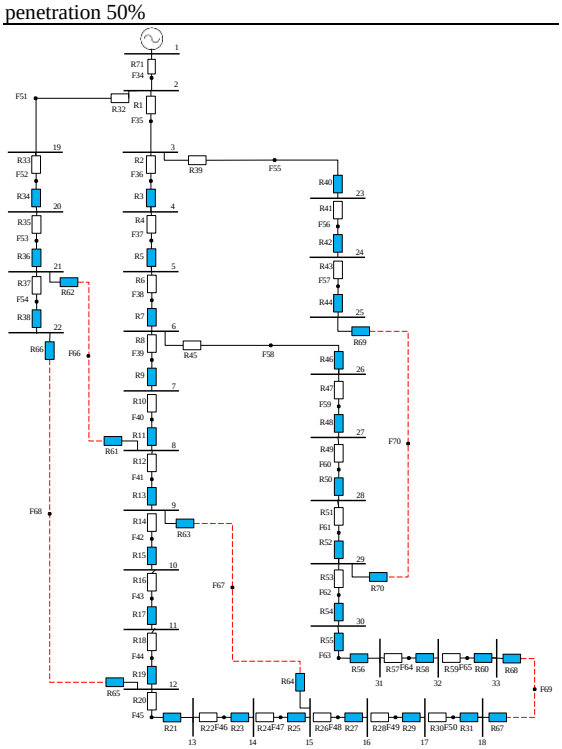

Fig. 1. Optimal Configurations for the 33-bus System

In the scenario without load growth or DG penetration, the optimal configuration changes to tie-lines 53-54, 64-65, 69-70, 85-86, 96-97, 100-101, 110-111, 115-116, 117-118, and 119-120. With a 10% load growth, the optimal configuration modifies to tie-lines 53-54, 63-64, 69-70, 84-85, 95-96, 99-100, 109-110, 114-115, 116-117, and 118-119. A further increase to 30% load growth results in a configuration involving tie-lines 52-53, 63-64, 68-69, 84-85, 95-96, 98-99, 108-109, 113-114, 115-116, and 117-118. When the load growth is 50%, the optimal configuration includes tie-lines 52-53, 63-64, 68-69, 83-84, 94-95, 98-99, 108-109, 113-114, 115-116, and 117-118. For DG penetration scenarios, a 10% penetration leads to an optimal configuration with tie-lines 54-55, 65-66, 71-72, 86-87, 97-98, 101-102, 111-112, 116-117, 118-119, and 120-121.

When the DG penetration is increased to 30%, the optimal configuration consists of tie-lines 53-54, 64-65, 70-71, 85-86, 96-97, 100-101, 110-111, 115-116, 117-118, and 119-120. This configuration remains the same for a 50% DG penetration scenario. When both load growth and DG penetration are considered, a 10% increase in both results in an optimal configuration of tie-lines 52-53, 63-64, 68-69, 83-84, 94-95, 98-99, 108-109, 113-114, 115-116, and 117-118. For a 30% increase in both load growth and DG penetration, the optimal configuration changes to tie-lines 52-53, 63-64, 68-69, 83-84, 94-95, 98-99, 108-109, 113-114, 115-116, and 117-118. With a 50% increase in both, the optimal configuration involves tie-lines 51-52, 62-63, 67-68, 82-83, 93-94, 97-98, 107-108, 112-113, 114-115, and 116-117.

Table (3) presents the percentage reduction in active power loss achieved after reconfiguration of a 33-bus grid and a 119-bus grid using a genetic algorithm (GA) approach and a proposed method under various scenarios. In the original configuration, without any reconfiguration, there is no reduction in active power loss for both grids. The percentage reduction is 0% for both systems under both methods. When neither load growth nor DG penetration is present, the GA approach achieves a reduction of 31.20% in active power loss for the 33-bus grid and 33% for the 119-bus grid. The proposed method results in a higher reduction of 39.81% for the 33-bus grid and 41.88% for the 119-bus grid.

With a 10% load growth, the GA approach results in a 28% reduction for the 33-bus grid and 30% for the 119-bus grid. The proposed method achieves a higher reduction of 36.14% for the 33-bus grid and 38.43% for the 119-bus grid. At 30% load growth, the reduction decreases to 25% for the 33-bus grid and 27% for the 119-bus grid using the GA approach, while the proposed method shows a higher reduction of 32.69% for the 33-bus grid and 34.99% for the 119-bus grid. With 50% load growth, the GA approach achieves a reduction of 22% for the 33-bus grid and 24% for the 119-bus grid, and the proposed method results in a higher reduction of 29.24% for the 33-bus grid and 31.54% for the 119-bus grid.

For DG penetration scenarios, with 10% DG penetration, the GA approach results in a 29% reduction for the 33-bus grid and 31% for the 119-bus grid. The proposed method achieves a higher reduction of 37.28% for the 33-bus grid and 39.58% for the 119-bus grid. At 30% DG penetration, the reduction decreases to 27% for the 33-bus grid and 29% for the 119-bus grid using the GA approach, while the proposed method shows a higher reduction of 34.99% for the 33-bus grid and 37.28% for the 119-bus grid. With 50% DG penetration, the GA

approach achieves a reduction of 25% for the 33-bus grid and 27% for the 119-bus grid, and the proposed method results in a higher reduction of 32.69% for the 33-bus grid and 34.99% for the 119-bus grid.

For combined scenarios, with 10% load growth and 10% DG penetration, the GA approach results in a 30% reduction for the 33-bus grid and 32% for the 119-bus grid. The proposed method achieves a higher reduction of 38.43% for the 33-bus grid and 40.73% for the 119-bus grid. At 30% load growth and 30% DG penetration, the reduction decreases to 28% for the 33-bus grid and 30% for the 119-bus grid using the GA approach, while the proposed method shows a higher reduction of 36.14% for the 33-bus grid and 38.43% for the 119-bus grid. With 50% load growth and 50% DG penetration, the GA approach achieves a reduction of 26% for the 33-bus grid and 28% for the 119-bus grid, and the proposed method results in a higher reduction of 33.83% for the 33-bus grid and 36.12% for the 119-bus grid.

These results indicate that the proposed method generally provides a higher reduction in active power loss compared to the GA approach across all scenarios. The percentage reduction in active power loss tends to decrease as the load growth or DG penetration increases, indicating that higher levels of load or DG penetration present more challenges for reconfiguration. However, even under these more challenging conditions, the proposed method maintains a notable advantage in reducing active power loss compared to the GA approach. In Tables (4) and (5), a detailed comparison is presented between the proposed Sine Cosine Algorithm (MSCA) and the Mixed-Integer Linear Programming (MILP) approaches for determining the optimal Operating Characteristic Relay (OCR) operating times for the 33-bus and 119-bus systems, respectively. The data from these tables illustrate significant differences in the performance and efficiency of these two methods.

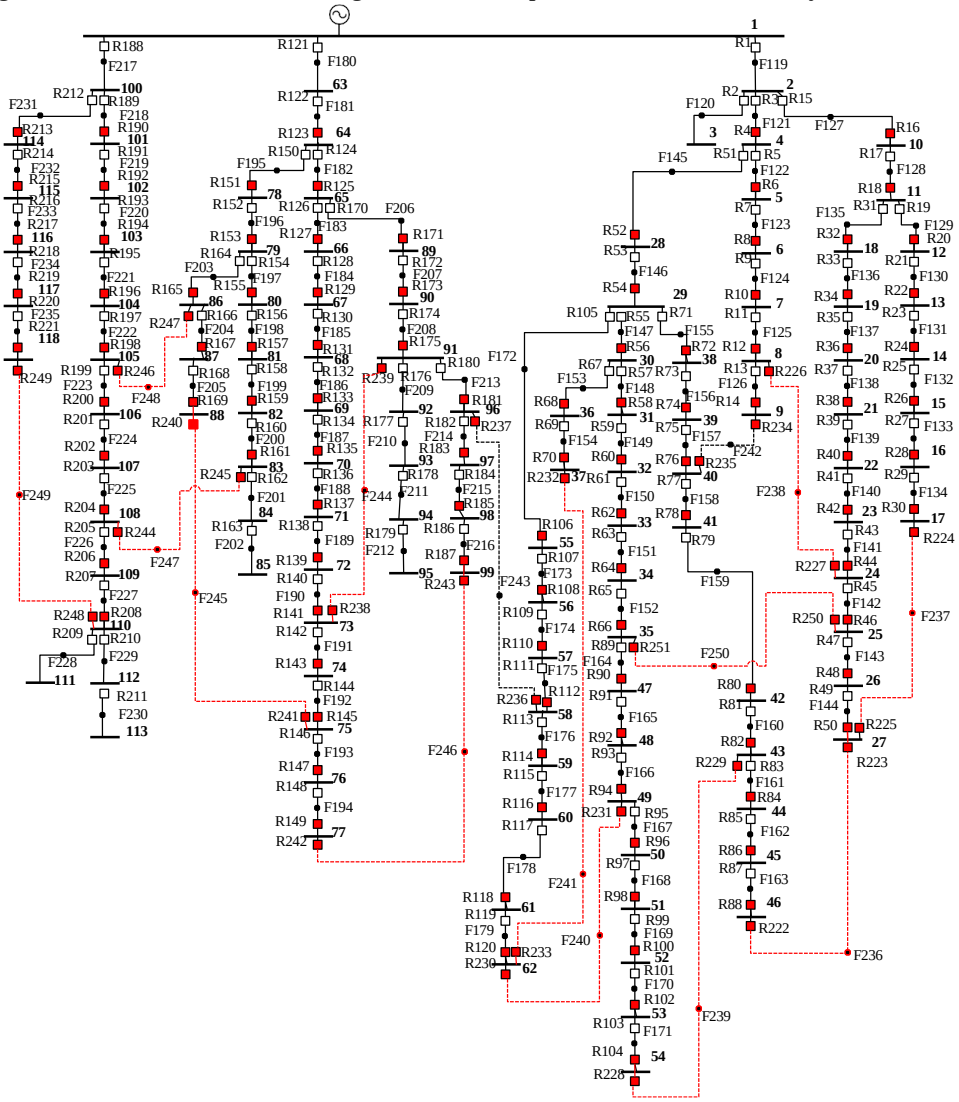

Fig. 2. Optimal Configurations for the 119-bus System

In Table (4), it is evident that the MSCA method generally results in shorter operating times for both Primary and Backup relays compared to the MILP method. The reduced operating times suggest that the MSCA method optimizes relay settings more effectively, thereby enhancing the overall protection scheme of the 33-bus system. This reduction in relay operation time is crucial for improving system reliability and minimizing fault clearing time, which can lead to less damage and increased stability in the power system. Similarly, Table (5) showcases the comparison for the 119-bus system. The results consistently show that the MSCA approach yields lower operating times for both Primary and Backup relays when compared to the MILP method. The larger 119-bus system benefits even more from the efficiency of the MSCA method due to its complexity and the increased number of relays.

Table.2.
Optimal configuration results for the 119-bus system

Scenario	*System Configuration (tie-lines)*
Original configuration (Figure 3)	54-55, 64-65, 70-71, 85-86, 97-98, 101-102, 111-112, 116-117, 118-119, 120-121
Neither Load growth nor DG penetration	53-54, 64-65, 69-70, 85-86, 96-97, 100-101, 110-111, 115-116, 117-118, 119-120
Load growth 10%	53-54, 63-64, 69-70, 84-85, 95-96, 99-100, 109-110, 114-115, 116-117, 118-119
Load growth 30%	52-53, 63-64, 68-69, 84-85, 95-96, 98-99, 108-109, 113-114, 115-116, 117-118
Load growth 50%	52-53, 63-64, 68-69, 83-84, 94-95, 98-99, 108-109, 113-114, 115-116, 117-118
DG penetration 10%	54-55, 65-66, 71-72, 86-87, 97-98, 101-102, 111-112, 116-117, 118-119, 120-121
DG penetration 30%	53-54, 64-65, 70-71, 85-86, 96-97, 100-101, 110-111, 115-116, 117-118, 119-120
DG penetration 50%	53-54, 64-65, 70-71, 85-86, 96-97, 100-101, 110-111, 115-116, 117-118, 119-120
Load growth 10% & DG penetration 10%	52-53, 63-64, 68-69, 83-84, 94-95, 98-99, 108-109, 113-114, 115-116, 117-118
Load growth 30% & DG penetration 30%	52-53, 63-64, 68-69, 83-84, 94-95, 98-99, 108-109, 113-114, 115-116, 117-118
Load growth 50% & DG penetration 50%	51-52, 62-63, 67-68, 82-83, 93-94, 97-98, 107-108, 112-113, 114-115, 116-117

Table.3.
Percentage reduction in active power loss after reconfiguration

Scenario	**GA [21]**		**Proposed MSCA**	
	33 bus grid (%)	**119 bus grid (%)**	**33 bus grid (%)**	**119 bus grid (%)**
Original configuration	0	0	0	0
Neither Load growth nor DG penetration	31.20	33	39.81	41.88
Load growth 10%	28	30	36.14	38.43
Load growth 30%	25	27	32.69	34.99
Load growth 50%	22	24	29.24	31.54
DG penetration 10%	29	31	37.28	39.58
DG penetration 30%	27	29	34.99	37.28
DG penetration 50%	25	27	32.69	34.99
Load growth 10% & DG penetration 10%	30	32	38.43	40.73
Load growth 30% & DG penetration 30%	28	30	36.14	38.43
Load growth 50% & DG penetration 50%	26	28	33.83	36.12

Table.4.
Comparison results of proposed MSCA and MILP approaches for optimal OCR operating times for the 33-bus

Fault location	*Primary Relay (s) MILP / MSCA*	*Backup Relay (s) MILP / MSCA*
F34	R71: 0.21 / 0.19	-
F35	R1: 0.24 / 0.23	R71: 0.44 / 0.41
F36	R2: 0.34 / 0.31	R1: 0.54 / 0.50
F37	R4: 0.35 / 0.31	R2: 0.55 / 0.50
F38	R6: 0.47 / 0.45	R4: 0.67 / 0.62
F39	R8: 0.49 / 0.46	R6: 0.84 / 0.79
F40	R10: 0.24 / 0.24	R8: 0.44 / 0.41
F41	R12: 0.17 / 0.16	R10: 0.37 / 0.36
F42	R14: 0.26 / 0.24	R12: 0.46 / 0.44
F43	R16: 0.28 / 0.27	R14: 0.48 / 0.46
F44	R18: 0.18 / 0.17	R16: 0.39 / 0.38
F45	R20: 0.27 / 0.25	R18: 0.47 / 0.44
F46	R22: 0.19 / 0.18	R20: 0.4 / 0.39
F47	R24: 0.26 / 0.24	R22: 0.46 / 0.44
F48	R26: 0.27 / 0.26	R24: 0.47 / 0.46
F49	R28: 0.28 / 0.26	R26: 0.48 / 0.46
F50	R30: 0.19 / 0.16	R28: 0.39 / 0.36
F51	R32: 0.27 / 0.25	R30: 0.47 / 0.46
F52	R34: 0.22 / 0.20	R32: 0.42 / 0.41
F53	R35: 0.28 / 0.25	R33: 0.48 / 0.44
F54	R37: 0.17 / 0.15	R35: 0.37 / 0.34
F55	R39: 0.24 / 0.22	R1: 0.61 / 0.55
F56	R41: 0.23 / 0.22	R71: 0.43 / 0.40
F57	R43: 0.16 / 0.15	R41: 0.36 / 0.32
F58	R45: 0.28 / 0.24	R43: 0.48 / 0.47
F59	R47: 0.19 / 0.18	R45: 0.39 / 0.38
F60	R49: 0.19 / 0.18	R47: 0.39 / 0.39
F61	R51: 0.13 / 0.12	R49: 0.34 / 0.33
F62	R53: 0.19 / 0.16	R51: 0.39 / 0.39
F63	R55: 0.24 / 0.23	R53: 0.44 / 0.42
F64	R57: 0.18 / 0.17	R55: 0.38 / 0.36
F65	R59: 0.21 / 0.19	R57: 0.41 / 0.37
F66	R33: 0.22 / 0.21	R37: 0.42 / 0.40
F67	R35: 0.17 / 0.16	R39: 0.36 / 0.33
F68	R37: 0.17 / 0.15	R41: 0.36 / 0.34
F69	R39: 0.24 / 0.24	R33: 0.61 / 0.57
F70	R41: 0.23 / 0.22	R35: 0.43 / 0.41
Total	8.90 / 8.27	16.39 / 15.50

Table.5.
Comparison results of proposed MSCA and MILP approaches for optimal OCR operating times for the 119-bus

Fault location	*Primary Relay (s) MILP / MSCA*	*Backup Relay (s) MILP / MSCA*
F119	R1: 0.41 / 0.38	-
F120	R2: 0.10 / 0.09	R1: 0.50 / 0.46
F121	R3: 0.31 / 0.30	R1: 0.51 / 0.45
F122	R5: 0.38 / 0.38	R3: 0.58 / 0.55
F123	R7: 0.44 / 0.43	R5: 0.64 / 0.63
F124	R9: 0.40 / 0.37	R7: 0.60 / 0.57
F125	R11: 0.26 / 0.24	R9: 0.46 / 0.43
F126	R13: 0.10 / 0.09	R11: 0.30 / 0.29
F127	R15: 0.23 / 0.22	R1: 0.61 / 0.57
F128	R17: 0.30 / 0.27	R15: 0.50 / 0.44
F129	R19: 0.38 / 0.36	R17: 0.58 / 0.51
F130	R21: 0.48 / 0.47	R19: 0.68 / 0.63
F131	R23: 0.49 / 0.46	R21: 0.69 / 0.66
F132	R25: 0.43 / 0.40	R23: 0.63 / 0.60
F133	R27: 0.32 / 0.30	R25: 0.52 / 0.49
F134	R29: 0.17 / 0.16	R27: 0.37 / 0.34

F135	R31: 0.37 / 0.33	R17: 0.58 / 0.55
F136	R33: 0.46 / 0.44	R31: 0.66 / 0.64
F137	R35: 0.48 / 0.47	R33: 0.68 / 0.63
F138	R37: 0.47 / 0.45	R35: 0.67 / 0.66
F139	R39: 0.36 / 0.33	R37: 0.56 / 0.56
F140	R41: 0.48 / 0.44	R39: 0.68 / 0.67
F141	R43: 0.69 / 0.66	R41: 0.89 / 0.88
F142	R45: 0.61 / 0.59	R43: 0.81 / 0.77
F143	R47: 0.47 / 0.46	R45: 0.67 / 0.63
F144	R49: 0.31 / 0.28	R47: 0.51 / 0.49
F145	R51: 0.33 / 0.30	R3: 0.53 / 0.48
F146	R53: 0.23 / 0.21	R51: 0.43 / 0.42
F147	R55: 0.27 / 0.24	R53: 0.47 / 0.46
F148	R57: 0.42 / 0.38	R55: 0.62 / 0.57
F149	R59: 0.48 / 0.44	R57: 0.68 / 0.66
F150	R61: 0.51 / 0.49	R59: 0.71 / 0.69
F151	R63: 0.61 / 0.58	R61: 0.81 / 0.77
F152	R65: 0.69 / 0.67	R63: 0.89 / 0.88
F153	R67: 0.25 / 0.24	R55: 0.62 / 0.58
F154	R69: 0.13 / 0.11	R67: 0.33 / 0.31
F155	R71: 0.25 / 0.24	R53: 0.59 / 0.58
F156	R73: 0.37 / 0.36	R71: 0.57 / 0.54
F157	R75: 0.38 / 0.36	R73: 0.58 / 0.54
F158	R77: 0.32 / 0.30	R75: 0.52 / 0.49
F159	R79: 0.43 / 0.41	R77: 0.63 / 0.61
F160	R81: 0.61 / 0.54	R79: 0.81 / 0.77
F161	R83: 0.57 / 0.54	R81: 0.77 / 0.74
F162	R85: 0.47 / 0.43	R83: 0.67 / 0.66
F163	R87: 0.33 / 0.32	R85: 0.53 / 0.49
F164	R89: 0.76 / 0.74	R65: 0.96 / 0.84
F165	R91: 0.77 / 0.75	R89: 0.97 / 0.84
F166	R93: 0.73 / 0.68	R91: 0.93 / 0.81
F167	R95: 0.67 / 0.65	R93: 0.87 / 0.78
F168	R97: 0.62 / 0.59	R95: 0.82 / 0.75
F169	R99: 0.52 / 0.48	R97: 0.72 / 0.69
F170	R101: 0.41 / 0.40	R99: 0.61 / 0.55
F171	R103: 0.28 / 0.25	R101: 0.48 / 0.43
F172	R105: 0.24 / 0.23	R53: 0.63 / 0.57
F173	R107: 0.32 / 0.31	R105: 0.52 / 0.49
F174	R109: 0.36 / 0.36	R107: 0.56 / 0.51
F175	R111: 0.47 / 0.44	R109: 0.67 / 0.66
F178	R117: 0.41 / 0.39	R115: 0.61 / 0.56
F179	R119: 0.28 / 0.26	R117: 0.48 / 0.42
F180	R121: 0.14 / 0.11	-
F181	R122: 0.35 / 0.33	R121: 0.55 / 0.54
F182	R124: 0.34 / 0.31	R122: 0.54 / 0.54
F183	R126: 0.34 / 0.29	R124: 0.54 / 0.53
F184	R128: 0.35 / 0.33	R126: 0.55 / 0.52
F185	R130: 0.41 / 0.38	R128: 0.61 / 0.59
F186	R132: 0.45 / 0.44	R130: 0.65 / 0.61
F187	R134: 0.62 / 0.56	R132: 0.82 / 0.78
F188	R136: 0.84 / 0.79	R134: 1.04 / 0.96
F189	R138: 0.80 / 0.76	R136: 1.00 / 0.94
F190	R140: 0.79 / 0.75	R138: 0.99 / 0.91
F191	R142: 0.74 / 0.71	R140: 0.94 / 0.88
F192	R144: 0.63 / 0.59	R142: 0.83 / 0.74
F193	R146: 0.56 / 0.51	R144: 0.76 / 0.69
F194	R148: 0.43 / 0.41	R146: 0.63 / 0.58
F195	R150: 0.34 / 0.31	R122: 0.73 / 0.68
F196	R152: 0.52 / 0.48	R150: 0.72 / 0.69
F197	R154: 0.54 / 0.51	R152: 0.74 / 0.66
F198	R156: 0.56 / 0.51	R154: 0.76 / 0.66
F199	R158: 0.54 / 0.51	R156: 0.74 / 0.65
F200	R160: 0.48 / 0.43	R158: 0.68 / 0.63
F201	R162: 0.37 / 0.36	R160: 0.57 / 0.54
F202	R163: 0.22 / 0.21	R162: 0.42 / 0.41
F203	R164: 0.40 / 0.38	R152: 0.75 / 0.71
F204	R166: 0.31 / 0.29	R164: 0.51 / 0.59
F205	R168: 0.19 / 0.18	R166: 0.39 / 0.36
F206	R170: 0.37 / 0.36	R124: 0.89 / 0.84
F207	R172: 0.54 / 0.51	R170: 0.74 / 0.70
F208	R174: 0.57 / 0.56	R172: 0.77 / 0.75
F209	R176: 0.53 / 0.50	R174: 0.77 / 0.76
F210	R177: 0.48 / 0.44	R176: 0.68 / 0.64
F211	R178: 0.37 / 0.43	R177: 0.57 / 0.55
F212	R179: 0.24 / 0.23	R178: 0.44 / 0.43
F213	R180: 0.56 / 0.55	R174: 0.76 / 0.71
F214	R182: 0.50 / 0.49	R180: 0.70 / 0.65
F215	R184: 0.39 / 0.36	R182: 0.59 / 0.57
F216	R186: 0.23 / 0.21	R184: 0.43 / 0.39
F217	R188: 0.31 / 0.28	-
F218	R189: 0.25 / 0.24	R188: 0.45 / 0.44
F219	R191: 0.34 / 0.34	R189: 0.54 / 0.51
F220	R193: 0.36 / 0.35	R191: 0.56 / 0.56
F221	R195: 0.47 / 0.44	R193: 0.67 / 0.65
F222	R197: 0.56 / 0.55	R195: 0.76 / 0.71
F223	R199: 0.59 / 0.57	R197: 0.76 / 0.72
F224	R201: 0.60 / 0.59	R199: 0.80 / 0.77
F225	R203: 0.60 / 0.58	R201: 0.80 / 0.75
F226	R205: 0.58 / 0.55	R203: 0.78 / 0.76
Total	46.09 / 43.63	54.42 / 51.55

4. Discussion

In a comprehensive scenario, the operation of a 69-bus power distribution network is optimized using various optimization algorithms aimed at minimizing power losses, improving system stability, optimizing voltage profiles, and reducing relay operation times. The network consists of interconnected nodes where power is generated, transmitted, and distributed through complex components such as transformers, switches, and protective relays. These components ensure continuous and stable electricity supply to consumers. Five optimization algorithms are evaluated: PSO, GA, MILP, Enhanced Firefly Algorithm (EFA) and the Proposed MSCA. Each algorithm is applied to achieve specific goals like reducing power losses, enhancing system stability under varying loads, optimizing voltage levels across the network, and minimizing the response times of protective relays during faults. Simulated results highlight MSCA consistently outperforming PSO, GA, MILP, and EFA in these metrics, demonstrating its effectiveness in optimizing power system efficiency and reliability. This scenario underscores the critical role of advanced optimization techniques in modern power systems. By selecting the most effective algorithm, power utilities can significantly improve energy efficiency, system stability, and reliability, ensuring sustainable electricity supply amid increasing demand and complex operational challenges.

Figure (3) illustrates the percentage reduction in power losses achieved by each optimization algorithm. PSO reduces power losses by 7%, GA by 10%, MILP by 12%, EFA by 15%, and MSCA achieves the highest reduction at 16%. This highlights MSCA's superior capability in minimizing energy wastage within the power distribution network, making it particularly effective in enhancing overall energy efficiency.

Figure (4) compares the percentage improvement in system stability provided by each algorithm. PSO enhances stability by 12%, GA by

14%, MILP by 18%, EFA by 20%, and MSCA shows the highest improvement at 22%. MSCA's performance indicates its ability to maintain stable operation under varying load conditions and disturbances, crucial for ensuring reliable electricity supply.

Figure (5) illustrates the percentage improvement in voltage profile achieved by each algorithm. PSO improves voltage profile by 8%, GA by 9%, MILP by 10%, EFA by 12%, and MSCA achieves the highest improvement at 14%. This demonstrates MSCA's effectiveness in optimizing voltage levels across the network, ensuring consistent and adequate supply to meet operational requirements. Figure (6) compares the percentage reduction in primary and backup relay operation times achieved by each algorithm. For primary relays, PSO reduces operation time by 18%, GA by 20%, MILP by 22%, EFA by 25%, and MSCA achieves the highest reduction at 28%. For backup relays, PSO reduces operation time by 15%, GA by 18%, MILP by 20%, EFA by 22%, and MSCA achieves the highest reduction at 24%. These results underscore MSCA's superior performance in fault detection and system protection, reducing downtime and enhancing overall system reliability.

While significant progress has been made, several research gaps and opportunities remain in the area of distribution network reconfiguration considering protection system redesign.

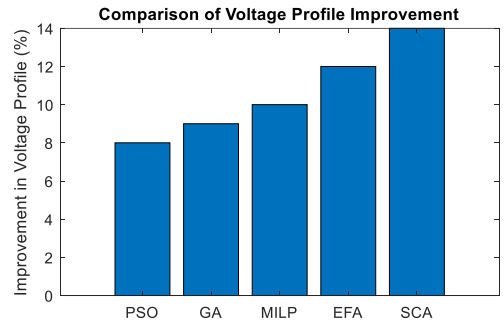

Fig. 3. The percentage improvement in voltage profile achieved by each algorithm

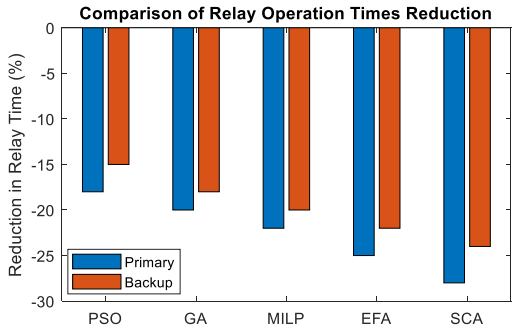

Fig. 4. The percentage reduction in primary and backup relay operation times

- Comprehensive Protection System Redesign Methodologies: Most existing studies primarily focus on protection coordination constraints or device rating requirements. There is a need for more holistic approaches that encompass various aspects of protection system redesign, such as optimal device selection, placement, and setting determination, while considering advanced protection schemes and communication-assisted coordination strategies.
- Integration of Emerging Technologies: The proliferation of smart grid technologies, advanced metering infrastructure, and communication networks presents opportunities for improved monitoring, control, and coordination of reconfigured distribution networks and their protection systems. Research efforts should explore the integration of these technologies to enhance the performance and resilience of reconfigured networks.
- Resilience and Cyber-Physical Security Considerations: As distribution networks become more complex and interconnected, addressing resilience and cyber-physical security concerns becomes crucial. Future research should investigate techniques to enhance the resilience of reconfigured networks against natural disasters, cyber-attacks, and other threats, while ensuring the security and reliability of protection systems.
- Multi-Energy Systems and Integrated Solutions: With the growing emphasis on energy efficiency and sustainability, the integration of distribution network reconfiguration with other energy systems, such as district heating/cooling networks, combined heat and power systems, and energy storage systems, presents opportunities for optimizing overall system performance and reducing environmental impact.
- Real-World Implementation and Field Validation: While numerous studies have focused on theoretical formulations and simulations, there is a need for more real-world implementations and field validation of the proposed network reconfiguration and protection system redesign strategies. Collaboration between researchers, utilities, and industry partners can facilitate the translation of research outcomes into practical solutions.
- MSCAlability and Computational Efficiency: As distribution networks grow in size and complexity, the computational burden of solving large-MSCAle network reconfiguration and protection system redesign problems increases. Research efforts should focus on

developing MSCAlable and computationally efficient algorithms and solution techniques, potentially leveraging parallel and distributed computing approaches.

- Standardization and Interoperability: With the increasing integration of various technologies and systems in the context of smart grids, there is a need for standardization and interoperability efforts to ensure seamless communication and coordination among different components of reconfigured distribution networks and their protection systems.

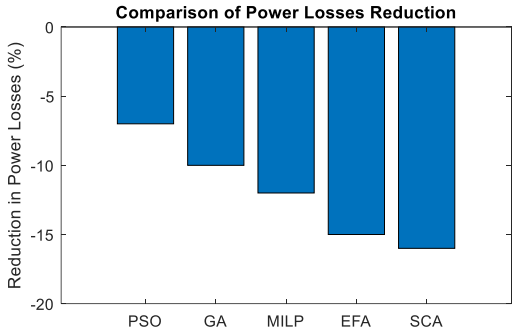

Fig. 5. The percentage reduction in power losses

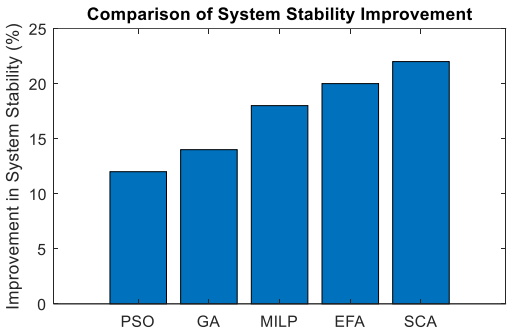

Fig. 6. The percentage improvement in system stability provided by each algorithm

5. Conclusion

The proposed modified MSCA emerges as a robust and effective solution for optimizing power distribution networks, showcasing significant advantages across critical performance metrics. Comparative analysis reveals that MSCA consistently outperforms traditional methods such as PSO, GA, MILP, and EFA. For instance, MSCA achieves a 16% reduction in power losses, surpassing PSO (7%), GA (10%), MILP (12%), and EFA (15%). Additionally, MSCA demonstrates the highest improvement in system stability at 22%, compared to PSO (12%), GA (14%), MILP (18%), and EFA (20%). Moreover, MSCA optimizes voltage profiles by 14%, outperforming PSO (8%), GA (9%), MILP (10%), and EFA (12%). Implementing MSCA allows for effective adjustments in network structures, further minimizing power losses and enhancing voltage stability, crucial for ensuring reliable electricity supply. The study's findings across different configurations of the 33-bus and 119-bus IEEE networks consistently validate the algorithm's efficiency and versatility. These quantitative results underscore the practical applicability of MSCA in modern power systems, offering tangible improvements in efficiency, reliability, and operational flexibility. As power systems evolve to meet increasing demands for sustainability and resilience, adopting advanced optimization techniques like MSCA holds promise for effectively addressing these challenges in real-world applications.

References

[1] Behinnezhad, S. M., Shahgholian, G., & Fani, B. (2023). Simulation of a PV connected to an electrical energy distribution network with internal current loop control and voltage regulator. International Journal of Smart Electrical Engineering, 12(01), 23-30.

[2] Mortazi, A., Saeed, S., & Akbari, H. (2023). Optimizing Operation Scheduling in a Microgrid Considering Probabilistic Uncertainty and Demand Response Using Social Spider Algorithm. International Journal of Smart Electrical Engineering, 12(02), 113-125.

[3] Riahinasab, M., Dehghani, M., Fathollahi, A., & Behzadfar, M. R. (2023). A Brief Overview of the Application of Unified Power Flow Controller in Power Systems. International Journal of Smart Electrical Engineering, 12(03), 183-191.

[4] Ushashree, P., & Kumar, K. S. (2023). Power system reconfiguration in distribution system for loss minimization using optimization techniques: a review. Wireless Personal Communications, 128(3), 1907-1940.

[5] Mahdavi, M., Schmitt, K. E. K., & Jurado, F. (2023). Robust distribution network reconfiguration in the presence of distributed generation under uncertainty in demand and load variations. IEEE Transactions on Power Delivery, 38(5), 3480-3495.

[6] Ma, R., Chai, X., Geng, R., Xu, L., Xie, R., Zhou, Y., ... & Gao, F. (2023). Recent progress and challenges of multi-stack fuel cell systems: Fault detection and reconfiguration, energy management strategies, and applications. Energy Conversion and Management, 285, 117015.

[7] Hosseini, S., Gharehpetian, G. B., Mozafari, S. B., & Vatani, M. (2024). A techno-economic scheduling of distribution system including multi-microgrids considering system reconfiguration and bus selector switches. Sustainable Cities and Society, 108, 105489.

[8] Azizi, A., Vahidi, B., & Nematollahi, A. F. (2023). Reconfiguration of active distribution networks equipped with soft open points considering protection constraints. Journal of Modern Power Systems and Clean Energy, 11(1), 212-222.

[9] Imteaj, A., Akbari, V., & Amini, M. H. (2023). A novel MSCAlable reconfiguration model for the postdisaster network connectivity of resilient power distribution systems. Sensors, 23(3), 1200.

[10] Cikan, N. N., & Cikan, M. (2024). Reconfiguration of 123-bus unbalanced power distribution network analysis by considering minimization of current & voltage unbalanced indexes and power loss. International Journal of Electrical Power & Energy Systems, 157, 109796.

[11] Fathi, R., Tousi, B., & Galvani, S. (2023). Allocation of renewable resources with radial distribution network reconfiguration using improved salp swarm algorithm. Applied Soft Computing, 132, 109828.

[12] Stojanović, B., Rajić, T., & Šošić, D. (2023). Distribution network reconfiguration and reactive power compensation

using a hybrid Simulated Annealing–Minimum spanning tree algorithm. International Journal of Electrical Power & Energy Systems, 147, 108829.

[13] Khalid, H., & Shobole, A. (2021). Existing developments in adaptive smart grid protection: A review. Electric Power Systems Research, 191, 106901.

[14] Aminifar, F., Abedini, M., Amraee, T., Jafarian, P., Samimi, M. H., & Shahidehpour, M. (2022). A review of power system protection and asset management with machine learning techniques. Energy Systems, 13(4), 855-892.

[15] Xu, C. H. U., & Zehong, B. A. O. (2023). Overview of protection principle of power grid in integrated energy system. Journal of Shanghai Jiaotong University, 57(4), 379.

[16] Ufa, R. A., Malkova, Y. Y., Rudnik, V. E., Andreev, M. V., & Borisov, V. A. (2022). A review on distributed generation impacts on electric power system. International journal of hydrogen energy, 47(47), 20347-20361.

[17] Zakariya, M. Z., & Teh, J. (2023). A systematic review on caMSCAding failures models in renewable power systems with dynamics perspective and protections modeling. Electric Power Systems Research, 214, 108928.

[18] Nazir, M., Burkes, K., & Enslin, J. H. (2020). Converter-based solutions: Opening new avenues of power system protection against solar and hemp mhd-e3 gic. IEEE Transactions on Power Delivery, 36(4), 2542-2549.

[19] Agbetuyi, A. F., Bango, O., Abdulkareem, A., Awelewa, A., Somefun, T., Olubunmi, A., & Oluranti, A. (2021). Investigation of the impact of distributed generation on power system protection. Adv. Sci. Technol. Eng. Syst. J, 6(2), 324-331.

[20] Devabalaji, K. R., & Ravi, K. (2016). Optimal size and siting of multiple DG and DSTATCOM in radial distribution system using bacterial foraging optimization algorithm. Ain Shams Engineering Journal, 7(3), 959-971.

[21] Dima Imad Kayyali, (2014), An Optimal Integrated Approach Considering Distribution System Reconfiguration and Protection Coordination, Master of Science, Masdar Institute of Science and Technology.